An In Vitro Mouse Model of Congenital Cytomegalovirus-induced Pathogenesis of the Inner Ear Cochlea

Michael Melnick and Tina Jaskoll

Laboratory for Developmental Genetics, University of Southern California, Los Angeles, California

Received 15 August 2012; Revised 22 October 2012; Accepted 6 November 2012

Congenital human cytomegalovirus (CMV) infection is the leading nongenetic etiology of sensorineural hearing loss (SNHL) at birth and prelingual SNHL not expressed at birth. The paucity of temporal bone autopsy specimens from infants with congenital CMV infection has hindered the critical correlation of histopathology with pathogenesis. Here, we present an in vitro embryonic mouse model of CMV-infected cochleas that mimics the human sites of viral infection and associated pathology. There is a striking dysplasia/hyperplasia in mouse CMV-infected cochlear epithelium and mesenchyme, including organ of Corti hair and supporting cells and stria vascularis. This is concomitant with significant dysregulation of *p19*, *p21*, *p27*, and *Pcna* gene expression, as well as proliferating cell nuclear antigen (PCNA) protein expression. Other pathologies similar to those arising from known deafness gene mutations include downregulation of KCNQ1 protein expression in the stria vascularis, as well as hypoplastic and dysmorphic melanocytes. Thus, this model provides a relevant and reliable platform within which the detailed cell and molecular biology of CMV-induced deafness may be studied. *Birth Defects Research (Part A) 97:69–78, 2013.* © 2012 Wiley Periodicals, Inc.

Key words: congenital cytomegalovirus infection; sensorineural hearing loss; in vitro mouse model; cochlear pathogenesis

INTRODUCTION

Congenital cytomegalovirus (CMV) infection is the leading cause of nongenetic birth defects, variably inducing hearing loss, blindness, and mental retardation (Fowler and Boppana, 2006; Pass et al., 2006; Schleiss and Choo, 2006; Pass, 2007; Schleiss, 2006, 2008; www.cdc.gov/cmv). Sensorineural hearing loss (SNHL) is the most frequent sequelae of in utero infection, accounting for 20 to 60% of all SNHLs. It is estimated that at least 8000 infants born annually in the United States will have congenital CMV-induced SNHL, at birth or later in early childhood. In newborns with congenital CMV infection, higher viral load at birth is consistently correlated with the presence of symptoms of congenital CMV and an elevated risk of SNHL; asymptomatic newborns have a lesser elevated risk (Cannon et al., 2011). Indeed, the cumulative risk of SNHL by age 8 is approximately 34% and 7% for populations of symptomatic and asymptomatic congenital CMV-infected children, respectively (Rosenthal et al., 2009). Thus, it is now well-established that congenital CMV infection is the major nongenetic cause of SNHL at birth and prelingual SNHL not expressed at birth (Barbi et al., 2003; Fowler and Boppana, 2006; Nance et al., 2006; Schleiss and Choo, 2006; Foulon et al., 2008a; Foulon et al., 2008b; Grosse et al., 2008; Cheeran et al., 2009).

Sensorineural hearing is mediated by the organ of Corti and associated structures in the scala media (SM), all of which sits inside the cochlear duct of the inner ear between the scala vestibuli (SV) and scala tympani (ST); the organ of Corti contains inner and outer mechanosensory hair cells embedded in a variety of supporting cells (Fig. 1A–C). Fluid-borne vibrations create a shearing vector in the stereocilia of the hair cells and subsequent signaling to the auditory cortex via the spiral ganglion and cochlear nerve.

Because of limited autopsy material, little is presently known about the underlying cochlear pathology of congenital CMV-induced SNHL. Nevertheless, what is known about the histopathology is quite instructive:

This research was supported by National Institute of Hospitals grant R21 DC010424 given to Tina Jaskoll and Michael Melnick.

Correspondence to: Tina Jaskoll, PhD, Laboratory for Developmental Genetics, University of Southern California, 925 W 34th Street, DEN 4264, MC-0641, Los Angeles, CA 90089-0641. E-mail: tjaskoll@usc.edu; and Michael Melnick, DDS, PhD, Laboratory for Developmental Genetics, University of Southern California, 925 W 34th Street, DEN 4266, MC-0641, Los Angeles, CA 90089-0641. E-mail: mmelnick@usc.edu

Published online 26 December 2012 in Wiley Online Library (wileyonlinelibrary.com).
DOI: 10.1002/bdra.23105

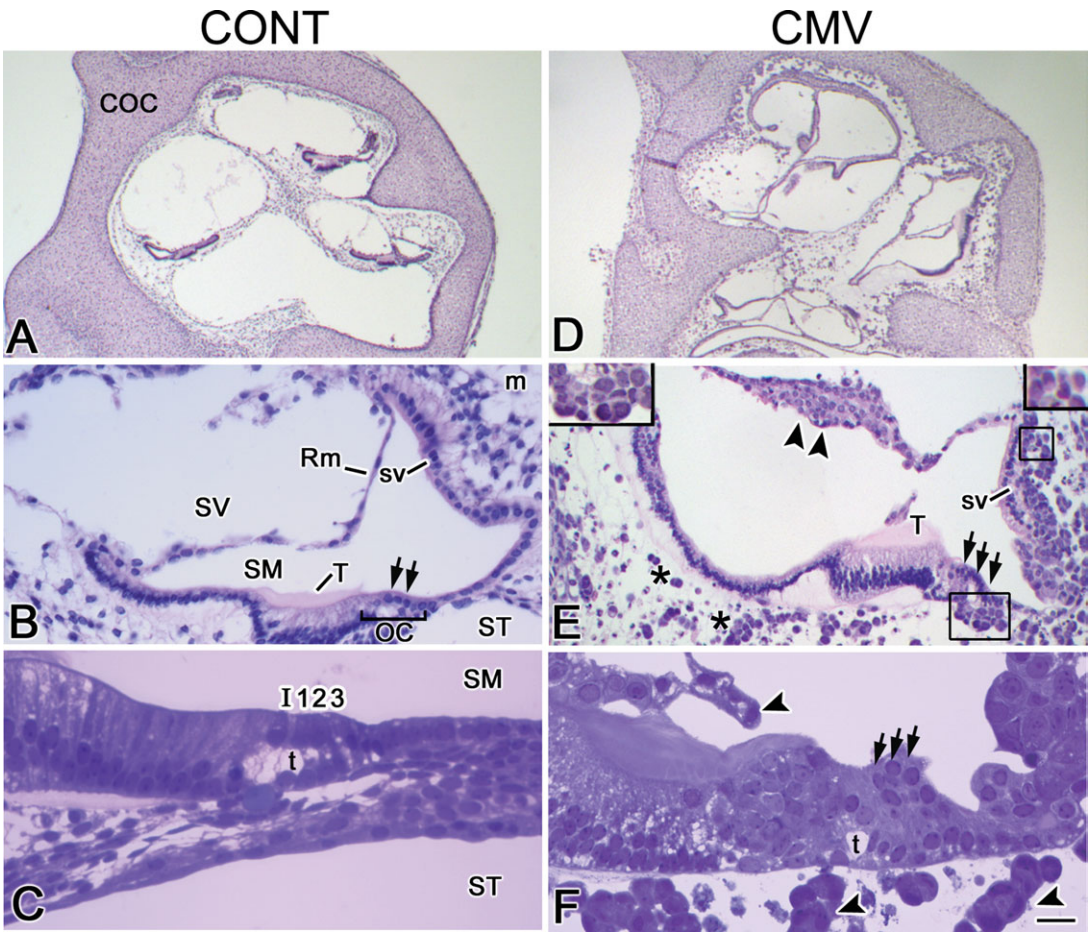

Figure 1. Mouse cytomegalovirus (mCMV) induces severely abnormal cochlear phenotypes. (**A, D**) Histologic sections through the basal, middle, and apical turns of the control (**A**) and mCMV-infected (**D**) embryonic day 15 (E15) cochlear ducts cultured for 12 days (E15 + 12). (**B, E**) Histology of paraffin-embedded control (**B**) and mCMV-infected (**E**) E15 + 12 cochleas. (**C, F**) Higher magnification of semithin plastic sections of control (**C**) and mCMV-infected (**F**) E15 + 12 cochleas. (**A–C**) In controls, the cochlear duct within the cartilaginous otic capsule (COC) is separated into scala vestibuli (SV), scala media (SM), and scala tympani (ST), each exhibiting distinct lumina. The organ of Corti (OC, *black bracket*) displays sensory (hair) (*double arrows*) and nonsensory (supporting) epithelial cells. Higher magnification (**C**) of organ of Corti showing the single inner hair cell (**I**) separated from the three outer hair cells (123) by the tunnel of Corti (t). Rm, Reissner's membrane; sv, stria vascularis; T, tectorial membrane. (**D–F**) The mCMV-infected cochleas are severely dysmorphic, exhibiting abnormal sensory (hair) (*triple arrows*) and nonsensory epithelia, Reissner's membrane (*double arrowheads*), and stria vascularis. Clusters of cytomegalic, basophilic, and pleiomorphic infected and affected cells are seen in Reissner's membrane (*double arrowheads*) and stria vascularis, as well as throughout the ST (**E**,*) and SV. Pathognomonic kidney shaped nuclei are seen in cells of Reissner's membrane (**F**, *arrowhead*), stria vascularis (**E**, right inset), and in mesenchymal cells found throughout SV and ST (**E**, left inset; **F**, *arrowheads*). Note the abnormal positioning of the tunnel of Corti in mCMV-infected cochleas (**F**). Bar: (**A, D**)-50 μm; (**B, E**)-30 μm; (**C, F**)-10 μm; (**E**) insets-15 μm.

degeneration or loss at birth of inner and outer hair cells, Reissner's membrane abnormalities, stria vascularis dysplasia, and labyrinthitis (Myers and Stool, 1968; Davis and Hawrisiak, 1977; Davis et al., 1977; Stagno et al., 1977; Davis, 1979; Davis, 1981; Strauss, 1990; Rarey and Davis, 1993; Schuknecht, 1993; Teissier et al., 2011). Further, viral inclusion bodies are found in the organ of Corti, Reissner's membrane, stria vascularis, and lining of the endolabyrinth (Myers and Stool, 1968; Davis et al., 1977; Davis, 1981; Teissier et al., 2011); viral antigens are immunodetected in the organ of Corti, Reissner's membrane, stria vascularis, and spiral ganglia (Stagno et al., 1977; Teissier et al., 2011). All this notwithstanding, the paucity of temporal bone autopsy specimens from infants with congenital CMV infection has hindered the critical correlation of pathology with mechanisms of CMV-induced SNHL (Davis, 1981; Strauss, 1990; Fowler and Boppana, 2006). Thus, there is a clear need for good animal models to investigate the histologic and molecular pathogenesis of CMV-induced SNHL.

Strict species-specificity of human CMV (hCMV) and the inability of species-specific rodent CMV to cross the placenta of mice and rats have hindered productive study of this virus in small animal models (Kern, 2006; Pass et al., 2006; Pass, 2007). To bypass the need for transplacental transmission of mouse CMV (mCMV), the mCMV has been directly injected into the fetus at midgestation or into the endometrial lumen of pregnant mice at the time of embryo implantation, respectively (Baskar et al., 1983; Baskar et al., 1987; Baskar et al., 1993; Tsut-

sui, 1995; Li and Tsutsui, 2000; Tsutsui et al., 2005). Although congenital embryonic abnormalities were reported, the high degree of fetal loss and difficulty in conducting these experiments limits the use of these in vivo mouse models for cell and molecular studies. Evidently, although the guinea pig (gp) is a well-studied model of transplacental viral transmission (Woolf, 1991; Kern, 2006; Schleiss and Choo, 2006; Schleiss, 2006, 2008), its use has been limited because of significant differences between human in utero CMV infection and the gpCMV congenital infection model, as well as differences between hCMV and gpCMV biologic characteristics (Kern, 2006; Schleiss and Choo, 2006; Pass, 2007). Clearly, alternative animal models are needed to delineate the cell and molecular mechanisms underlying CMV-induced cochlear pathogenesis.

A useful and relevant animal model has always to be informed by two key clinical observations: (1) in utero CMV infection causes SNHL, whereas postnatally acquired infection in premature infants does not (Vollmer et al., 2004); (2) SNHL is more common in infants with congenital CMV infection resulting from first trimester maternal infection than when infection takes place later in pregnancy (Pass et al., 2006; Foulon et al., 2008a; Foulon et al., 2008b). Both of these findings highlight the need to investigate the mechanisms of CMV-induced cochlear pathogenesis in embryonic organs. To this end, we have developed an in vitro embryonic mouse model of CMV-induced pathogenesis that mimics the known human pathology, including dysplasia of the organ of Corti, Reissner's membrane, and stria vascularis. This model will prove useful in studying the CMV-induced dysregulation of signaling pathways during early and late stages of cochlear morphogenesis.

MATERIALS AND METHODS

Animals

Timed pregnant inbred C57/BL6 female mice were purchased from Charles River (Wilmington, MA; plug day = day 0 of gestation) and embryonic day 15 (E15) fetuses were harvested as previously described (Melnick et al., 2006). All protocols involving mice were approved by the Institutional Animal Care and Use Committee (USC, Los Angeles, CA).

Organ Culture

Whole inner ears were dissected of E15 mouse fetuses and the ventral cochlear region and dorsal vestibular region were separated. Cochleas were cultured using a modified otic organ culture system first described by Van de Water and Ruben (1971) and chemically defined BGJb medium (Invitrogen Corporation, Carlsbad, CA) supplemented with 10% fetal calf serum, 0.5 mg ascorbic acid/mL, and 50 units/mL penicillin/streptomycin (Invitrogen Corporation), pH 7.2, as previously described (Melnick et al., 2006). We cultured the cochlear duct with surrounding periotic mesenchyme because prior studies have demonstrated cochlear morphogenesis and hair cell differentiation are dependent on a complex series of interactions between otic epithelia and periotic mesenchyme (e.g., Van de Water and Represa, 1991; Doetzlhofer et al., 2004; Xu et al., 2007) and CMV seems to primarily infect embryonic mesenchyme (Melnick et al., 2006; Jaskoll et al., 2008a; Jaskoll et al., 2008b). For mCMV infection, cochleas were incubated with 1×10^{-5} plaque-forming units (PFU)/mL of *lacZ*-tagged mCMV RM427+ in BGJb on day 0 for 24 hours and then cultured in virus-free media; controls consisted of cochleas cultured in control medium for the entire period. Cochleas were collected and processed for hematoxylin and eosin histology, quantitative RT-PCR (qRT-PCR), immunolocalization, or cell proliferation (proliferating cell nuclear antigen [PCNA]) analysis. For qRT-PCR, four to five cochleas were pooled, snap frozen, and stored at −80°C. For histology, immunolocalization, and PCNA analyses, cochleas were fixed for 4 hours in Carnoy's fixative or overnight in 4% paraformaldehyde at 4°C, embedded in paraffin, serially sectioned at 8 μm, and stained as previously described (Melnick et al., 2006). For β-galactosidase staining, cochleas were fixed in 0.2% gluteraldehyde, stained, and processed, as previously described (Melnick et al., 2006). For semi-thin sections, E15 + 12 cochleas were fixed overnight in 10% neutral buffered formalin at 4°C, embedded in JB-4 resin according to the JB-4 embedding kit (Polysciences, Inc, Warrington, PA), sectioned at 1 μm, and stained with 1% toluidine blue.

mCMV Distribution

We assayed β-galactosidase (*lacZ*) activity and localization of viral immediate early (IE1) proteins, as described in Melnick et al. (2006). For β-galactosidase staining: briefly, mCMV-infected E15 + 6, E15 + 9, and E15 + 12 cochleas were processed, stained for 4 to 6 hours, and photographed. Whole mounts were then dehydrated through graded alcohols, embedded in paraffin, serially sectioned at 8 μm, and counterstained with eosin. For IE1 distribution: mCMV-infected E15 + 6, E15 + 9, and E15 + 12 cochleas were embedded in low melting point paraplast, serially sectioned, and incubated overnight with antimouse IE1 antibodies (kindly provided by Dr. Edward Mocarski, Emory University); controls consisted of sections incubated in the absence of primary antibody. For each experimental protocol, a minimum of three to five explants/day were analyzed.

Immunolocalization

Cultured cochleas were embedded in low melting point paraplast, serially sectioned, and immunostained essentially as described in Melnick et al. (2006 and 2011) using the following commercially available antibodies: myosin-VI (Proteus Biosciences, Inc, Ramona, CA; cat. #25-6791); myosin-VIIa (Proteus Biosciences, cat. #25-6790); and KCNQ1 (Santa Cruz Biotechnology, Santa Cruz, CA; cat. #sc-20816). Nuclei were counterstained with DAPI (Invitrogen Corporation). Negative controls were performed in parallel under identical conditions and consisted of sections incubated without primary antibodies. For each treatment group, three to five explants per day per antibody were analyzed. All images in this study were acquired with a Zeiss Axioplan microscope (Carl Zeiss Group, Oberkochen, Germany) equipped with a SPOT RT3 camera and processed with SPOT Advanced (Spot Imaging Solutions, Sterling Heights, MI) and Adobe Photoshop CS2 software (Adobe Systems Incorporated, San Jose, CA).

Cell-specific Distribution of PCNA

The cell-specific localization of PCNA was determined using the Zymed mouse PCNA kit (Invitrogen Corporation) and counterstained with hematoxylin, as previously described (Melnick et al., 2006); the cytoplasm stains blue and PCNA-positive nuclei stains dark brown. In this set of experiments, three to eight cultures per treatment per day were analyzed.

PCNA immunolocalization is frequently used as a surrogate marker of cell division (e.g., Chen and Segil, 1999; Melnick et al., 2006; Melnick et al., 2011; von Bohlen und Halbach, 2011), notably because it is the ''maestro'' of the DNA replication fork (Moldovan et al., 2007). High fidelity genome duplication is assured through a collection of dynamic PCNA-containing protein complexes at the fork (Kirchmaier, 2011). During DNA replication, PCNA is loaded onto DNA at the 3′ ends of primer-template junctions and acts as a sliding clamp that interacts with and enhances the efficiency of the DNA polymerases on the leading and lagging DNA strands (Kirchmaier, 2011). Thus, because PCNA is central to successful DNA replication, PCNA is a well-recognized surrogate cell division marker (von Bohlen und Halbach, 2011). Although the sensitivity of this immunoassay approaches 100%, the specificity may be variably reduced because PCNA is also essential for DNA repair and its relatively long half-life (8–20 hours) results in some presence in early G_o (Zacchetti et al., 2003). This may result in an overestimation of the fraction of cells actually dividing.

Quantitative RT-PCR

For analysis of gene expression, qRT-PCR was conducted, as previously described (Melnick et al., 2006; Melnick et al., 2009), on E15 + 6, E15 + 9, and E15 + 12 control, and mCMV-infected samples; each sample consisted of four to five pooled explants. RNA was extracted and 1 μg RNA was reverse transcribed into first strand cDNA using ReactionReady First Strand cDNA Synthesis Kit: C-01 for reverse transcription (SABiosciences, Frederick, MD). The primer sets used were prevalidated to give single amplicons and purchased from SABiosciences: Kcnq1 (PPM04198A); p19 (Cdkn2d; cat. #PPM02987A); p21 (Cdkn1a; cat. #PPM02901A); p27 (Cdkn1b; cat. #PPM02909A); and Pcna (cat. #PPM03456A). Primers were used at concentration of 0.4 microM. The cycling parameters were 95°C, 15 minutes; 40 cycles of (95°C, 15 seconds; 55°C, 30–40 seconds and 72°C, 30 seconds). Specificity of the reactions was determined by subsequent melting curve analysis. RT-PCRs of RNA (not reverse transcribed) were used as negative controls. GAPDH was used to control for equal cDNA inputs and the levels of PCR product were expressed as a function of GAPDH. The relative fold changes of gene expression between the gene of interest and GAPDH, or between the E15 + 6, E15 + 9, and E15 + 12 control and mCMV-infected samples, were calculated by the $2^{-\Delta\Delta CT}$ method. Significant expression differences between mCMV-infected and control samples were determined by *t* test, with $\alpha = 0.01$ and the null hypothesis of $R = 1$, where R is the mean relative expression ration (mCMV/control) across the entire sample ($n = 9$). Expression ratios were log transformed before analysis to satisfy the assumption of normality.

RESULTS

mCMV, having many features in common with hCMV, has been widely used for studying the postnatal pathogenesis associated with acute, latent, and recurrent infections (Krmpotic et al., 2003; Cheeran et al., 2009); the mouse is the most comprehensive model system for the developing mammalian cochlea (Kelley, 2007; Driver and Kelley, 2009; Puligilla and Kelley, 2009). Here, we developed an embryonic mouse organ culture model to study the effect of mCMV on embryonic cochlear development. Specifically, we infected E15 cochleas with *lac*Z-tagged mCMV for up to 12 days in vitro, as previously described (Melnick et al., 2006; Jaskoll et al., 2008a; Jaskoll et al., 2008b) using a modified Van de Water and Ruben (1971) organ culture system; controls were cultured in virus-free, chemically defined media. mCMV-infected cochleas are developmentally delayed and exhibit severely abnormal phenotypes (Figs. 1–5).

In controls, cochlear morphogenesis and histodifferentation progresses normally in vitro (Fig. 1A–C). The cochlear duct is separated into the SV, SM, and ST; the organ of Corti, located on the floor of the SM, is characterized by differentiating epithelial sensory hair cells and nonsensory supporting cells (Fig. 1B, C). Differentiating hair cells can be identified based on position, an increase in nuclei size, a more luminal position of their nuclei, and expression of myosin VI and VIIa, cytoplasmic hair cell-specific markers (Hasson et al., 1995; Hasson et al., 1997). In controls, the organ of Corti displays three outer hair cells and one inner hair cell (Figs. 1B, C; and 2A).

mCMV infection of E15 cochleas induces a severely dysmorphic and dysplastic phenotype in the organ of Corti, Reissner's membrane, stria vascularis, ST, and SV (Fig. 1D–F). Cytomegalic, basophilic, and pleomorphic cells (some with viral inclusion bodies) are found in Reissner's membrane and stria vascularis (Fig. 1E, F). The sensory (hair) and nonsensory (supporting) epithelial cells of the organ of Corti are severely disorganized (Fig. 1E, F); significantly, mCMV seems to induce a hair cell hyperplasia that is densely packed and misaligned (Fig. 2B). mCMV infection also induces substantial differences in the periotic mesenchyme that surrounds the forming ST and SV, namely the presence of basophilic, cytomegalic cells (Fig. 1E, F). Coincident with the presence of pathognomonic kidney shaped nuclei (Fig. 1E insets, F), *lac*-Z-tagged mCMV (Fig. 3A), and viral IE1 (immediate early 1) protein (Fig. 3B) are clearly evident in Reissner's membrane, stria vascularis, ST, and SV, and less so in the organ of Corti. Finally, it should be noted that near simultaneous administration of the antiherpes viral nucleoside, acyclovir, with mCMV infection obviates all cochlear abnormality (data not shown), as is the case with other developing organs previously studied (Melnick et al., 2006; Jaskoll et al., 2008a; Jaskoll et al., 2008b; Melnick et al., 2011).

Dysregulation of the Cell Cycle

Given that (1) mCMV infection has repeatedly been shown to induce cell proliferation and to concomitantly dysregulate the gene and protein expression of numerous components of the cell cycle (Hertel and Mocarski, 2004; Melnick et al., 2006; Hertel et al., 2007; Melnick et al., 2011), and (2) withdrawal from the cell cycle is a

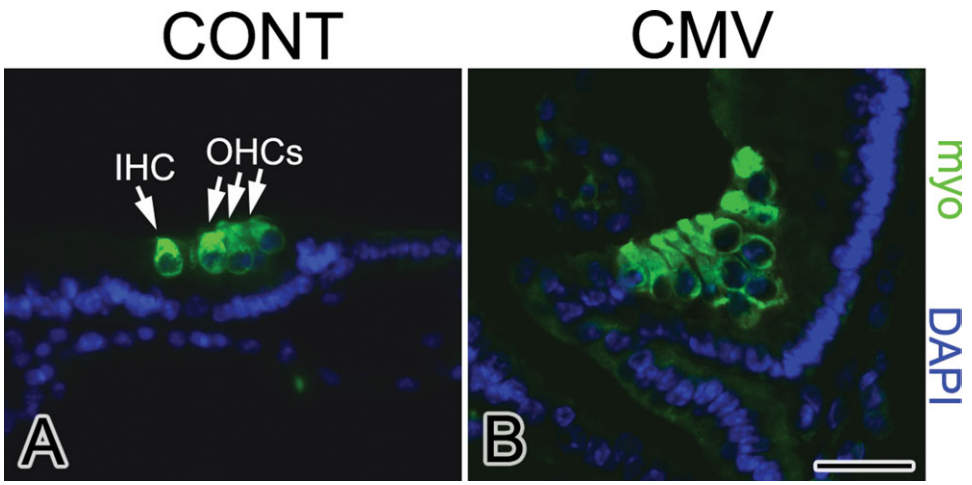

Figure 2. Mouse cytomegalovirus (mCMV) induces a dramatic dysplasia/hyperplasia of hair cells. CONT (**A**) and mCMV-infected (**B**) embryonic day 15 (E15) + 12 cochleas. Hair cells are labeled with an antibody to myosin (myo, green); nuclei are stained with DAPI (blue). Controls (**A**) display one inner hair cell (IHC) and three outer hair cells (OHCs) properly aligned. mCMV (**B**) induces a notable increase in hair cell population; this expanded hair cell population is densely packed and disorganized. (**A, B**)-50 μm.

prerequisite of organ of Corti histodifferentation (Ruben, 1967; Chen and Segil, 1999; Laine et al., 2007), we compared the cell-specific distribution of PCNA, an E2F/DP target gene during the S-phase of active cell division (Chen and Segil, 1999; Melnick et al., 2006), in infected and uninfected E15 cochleas cultured for 6 (E15 + 6), 9 (E15 + 9), and 12 (E15 + 12) days (Fig. 4). A dramatic increase in PCNA-positive nuclei is seen in mCMV-infected and affected cochlear mesenchymal and epithelial cells, including apparent nonsensory, supporting epithelial cells of the organ of Corti (compare Fig. 4B, D, F to 4A, B, C); the variability of PCNA expression is time dependent (compare Fig. 4B, D, and F). The results are consistent with the evolving hyperplasias and dysplasias noted above (Figs. 1 and 2).

Cyclin-dependent kinase (Cdkn) inhibitors are critical gatekeepers of S-phase entry in the cell cycle; they bind to and inhibit cyclin-dependent kinase/cyclin complexes, and thus inhibit cell proliferation. Inhibitors p19 (Cdkn2d) and p21 (Cdkn1a) and inhibitor p27 (Cdkn1b) serve to regulate the number of hair cells and supporting cells, respectively (Chen and Segil, 1999; Laine et al., 2007). The qRT-PCR reveals the time-dependent changes in *p19*, *p21*, and *p27* gene expression relative to *Pcna* gene expression (Table 1). At E15 + 6, there is a highly significant ($p < 0.001$) drop in *p19* and *p27* expression but a near 50% increase in *p21* ($p < 0.01$); there is a modest but significant ($p < 0.001$) increase in *Pcna*. Although *p19* and *p27* expression rebounds across postinfection days 9 and 12, there remains a highly significant ($p < 0.001$) 2.5 to 3-fold increase in *Pcna* expression; this is consistent with the common lag between gene transcription and protein translation. The correlation and timing of *Cdkn* downregulation and *Pcna* upregulation with upregulation of

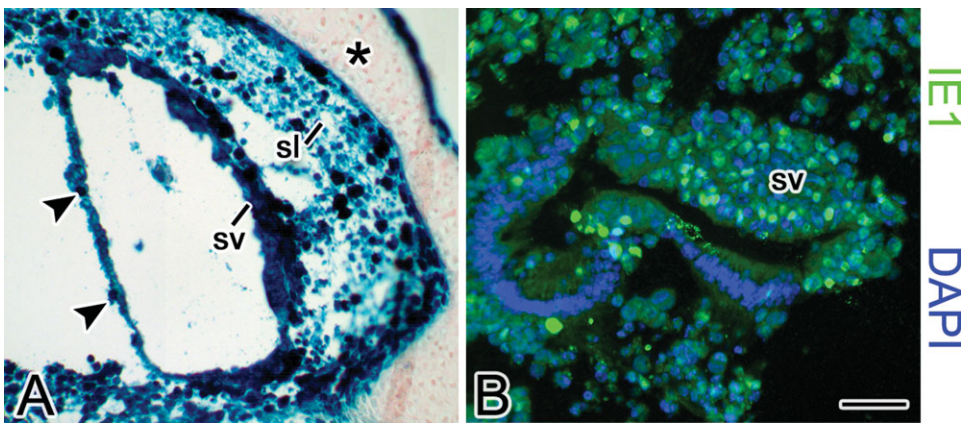

Figure 3. Distribution of viral infection in mouse cytomegalovirus (mCMV)-infected cochleas. (**A**) β-galactosidase-stained histologic section of an embryonic day 15 (E15) cochlea cultured in the presence of *lacZ*-tagged mCMV for 9 days. (**B**) Immunolocalization of viral IE1 proteins in an mCMV-infected cochlea cultured for 12 days. mCMV and viral IE1 proteins are primarily seen in the stria vascularis (sv), Reissner's membrane (*arrowheads*), spiral ligament (sl), and surrounding periotic mesenchyme, and more sparsely in the organ of Corti. Note that virus is absent from the cartilaginous otic capsule (**A**, *). Bar: (**A**)-50 μm; (**B**)-35 μm.

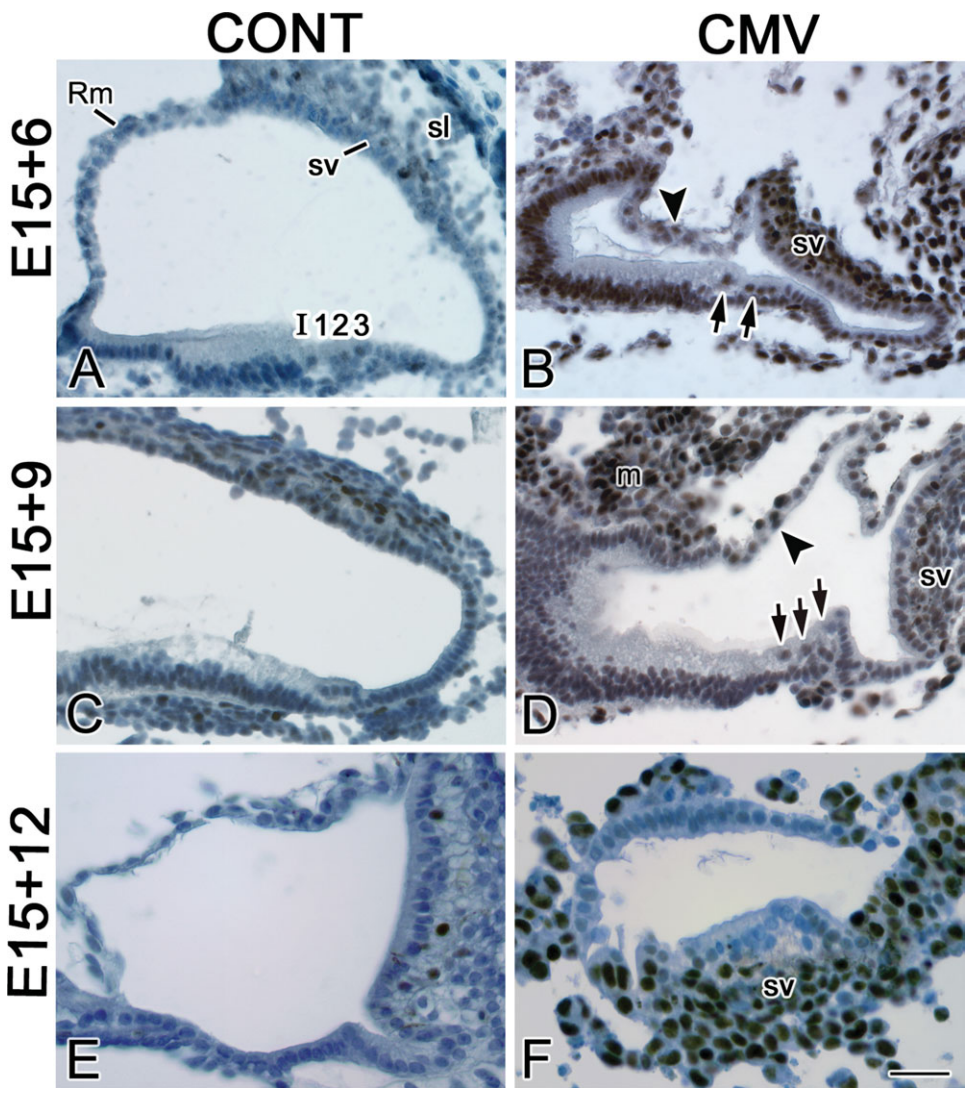

Figure 4. Mouse cytomegalovirus (mCMV) induces a notable increase in proliferating cell nuclear antigen (PCNA)-positive nuclei in mCMV-infected cochleas on days 6, 9, and 12 of culture. In embryonic day 15 (E15) + 6 (**A**), E15 + 9 (**C**), and 15 + 12 (**E**) controls, PCNA-positive nuclei (brown) are relatively absent. Note the absence of PCNA-positive nuclei in the single inner hair cell (I), the three outer hair cells (123) and epithelial nonsensory supporting cells. In contrast, mCMV-infected E15 + 6 (**B**), E15 + 9 (**D**), and E15 + 12 (**F**) cochleas exhibit a dramatic increase in PCNA-positive nuclei in infected and affected cells. In E15 + 6 cochleas, PCNA-positive nuclei are seen in the relatively normal appearing single inner hair and three outer hair cells (*double arrows*), as well as throughout cochlear epithelia, stria vascularis (sv), Reissner's membrane (*arrowhead*), and abnormal periotic mesenchyme. By days 9 (E15 + 9) (**D**) and 12 (E15 + 12) (**E**) of culture, the mCMV-infected cochleas seem more severely abnormal. On day 9 (**D**), PCNA-positive nuclei are found in the hair cells (*triple arrows*) of the dysmorphic organ of Corti, Reissner's membrane (*arrowhead*), the stria vascularis (sv), spiral ligament, and in the cytomegalic, basophilic mesenchymal cells (m) found throughout the scala vestibuli (SV) and scala tympani (ST). On day 12 (**F**), PCNA-positive nuclei are primarily seen in the stria vascularis and are mostly absent from the cochlear epithelial cells. Bar: (**A–D**)-30 μm; (**E, F**)-50 μm.

PCNA protein informs the mechanism of cochlear hyperplasia.

Stria Vascularis Dysplasia

The stria vascularis is composed of three cell layers (Kikuchi and Hilding, 1966; Jin et al., 2007). The marginal cells face the lumen of the SM and are characterized by numerous mitochondria and extensive membrane infolding; the intermediate cells are neural crest-derived melanocytes; the basal cells are characterized by tight junctions and serve as a barrier between the stria vascularis and the adjacent spiral ligament. The stria vascularis of mCMV-infected E15 + 12 cochleas are severely dysplastic (Figs. 1 and 5). The cells of all three layers are greatly enlarged and misaligned, making clear distinction of the layers difficult. With mCMV infection, many of the cytomegalic cells contain pathognomonic kidney shaped nuclei (Fig. 5B) and viral IE1 protein (Fig. 5B, left inset); the melanocytes are reduced in number and dysmorphic

Table 1
mCMV Modulation of Embryonic Cochlear Gene Expression

	Days post-infection (E15 + x)					
	E15 + 6		E15 + 9		E15 + 12	
Gene	R	η	R	η	R	η
p19	0.60^{**}	0.15	0.85^{*}	0.15	1.37^{**}	0.10
p21	1.46^{*}	0.25	1.48^{**}	0.14	1.12^{ns}	0.12
p27	0.55^{**}	0.18	0.76*	0.21	0.94^{ns}	0.22
Pcna	1.34^{**}	0.08	3.09^{**}	0.13	2.47^{**}	0.17
Kcnq1	0.23^{**}	0.26	0.42^{**}	0.05	0.31^{**}	0.23

R = mean relative expression ratio = mCMV/control (n = 9).
η = gene expression noise (0→1) = s_R/R (where s_R = SD of R).
$^{*}p < 0.01$;
$^{**}p < 0.001$; ns = not significant ($p > 0.01$). mCMV, mouse cytomegalovirus; E15, embryonic day 15.

(Fig. 5B, right inset). Finally, there is a marked downregulation of potassium channel KCNQ1 protein in the marginal cells of the mCMV-infected stria vascularis (compare Fig. 5D to C). This is concomitant with a highly significant ($p < 0.001$) and dramatic 60 to 75% decline in *Kcnq1* gene expression across all days of infection (Table 1).

DISCUSSION

As noted above, congenital hCMV infection is the leading nongenetic etiology of SNHL at birth and prelingual SNHL not expressed at birth (Fowler and Boppana, 2006; Nance et al., 2006; Grosse et al., 2008). Limited human temporal bone autopsy investigation reveals an instructive correlation of pathognomonic kidney shaped nuclei and viral antigens in the organ of Corti, Reissner's membrane, and stria vascularis, with aplasia/hyperplasia of hair cells, as well as dysplasia of Reissner's membrane and stria vascularis (Myers and Stool, 1968; Davis and Hawrisiak, 1977; Davis et al., 1977; Stagno et al., 1977; Davis, 1979; Davis, 1981; Strauss, 1990; Rarey and Davis, 1993; Schuknecht, 1993; Teissier et al., 2011). Here, we present an in vitro embryonic mouse model of CMV-infected cochleas that mimics the human sites of viral infection and associated pathology (Figs. 1–5). Further, it provides initial insight into the likely cell and molecular pathogenesis of the resultant hearing loss (Figs. 4 and 5; Table 1).

In general, mCMV infection induces a severely dysmorphic embryonic cochlear phenotype, including hyperplasia and dysplasia in the organ of Corti, Reissner's membrane, stria vascularis, SV, and ST. Several findings are of particular note: hyperplasia of hair cells; downregulation of KCNQ1 protein expression in the stria vascularis; hypoplastic and dysmorphic melanocytes.

Organs of Corti in mCMV-infected cochleas are characterized by hyperplasia and malalignment of sensory (hair) and nonsensory (supporting) epithelium (Figs. 1 and 2). The organ of Corti develops from a subset of epithelial cells occupying the floor of the cochlear duct; by E14.5, this prosensory domain becomes totally postmitotic and terminal histodifferentiation commences; by E17, differentiated hair cells and supporting cells have arranged themselves into a nectin-dependent checkerboard-like pattern along the entire length of the cochlear duct (Kelley, 2007; Togashi et al., 2011). Withdrawal from the cell cycle is critical to the proper histodifferentation; maintaining withdrawal is critical to the morphologic and functional integrity of the organ of Corti (Ruben, 1967). Important to this cell cycle inhibition are the cyclin-dependent kinase inhibitors p19, p21, and p27 (Chen and Segil, 1999; Chen et al., 2003; Laine et al., 2007).

The embryonic organ culture model shows a dramatic increase in immunolocalized PCNA, a surrogate S-phase marker of cell division, in mCMV-infected cochlear epithelium and mesenchyme, including the cells in the organ of Corti (Fig. 4). This is concomitant with significant changes in *p19*, *p21*, *p27*, and *Pcna* gene expression (Table 1). Inter alia, downregulation of cdk-inhibitors results in S-phase entry, upregulation of *Pcna* expression, and increased cell division. The patterns of expression through in vitro stages equivalent to perinatal (E15 + 6) and early postnatal (E15 + 9, E15 + 12) cochlear development are instructive: *p19* and *p27* are dramatically lower at E15 + 6, less so at E15 + 9, and normal or elevated at E15 + 12; *p21* is significantly elevated at E15 + 6 and E15 + 9, but returns to normal with the recovery of *p19* and *p27* at E15 + 12; *Pcna* transcript is significantly elevated throughout.

Although p21 has been shown to compensate for p19 deletion (Laine et al., 2007), upregulation of p21 seems to have little effect upon the delayed withdrawal from or re-entry to the cell cycle of cells in the prosensory domain well into the modeled early postnatal period. Still, the fact that by E15 + 12 all three cdk-inhibitors are at or above control levels suggests that the prosensory epithelium is about to withdraw from the cell cycle shortly. Finally, it is clear that by E15 + 12 there is a well-defined population of excessive and disorganized hair cells (Figs. 1F and 2B). What is not clear is whether these cells result from continued proliferation of sensory epithelium or transdifferentiation from proliferating nonsensory epithelium or both. Also not known is whether the apparent increased number of hair cells is transient and will succumb to subsequent p53-mediated apoptosis as seen with p19 and p21 deletions (Chen et al., 2003; Laine et al., 2007). What is certain is that malalignment or loss of sensory hair cells is not compatible with normal hearing.

The stria vascularis of mCMV-infected cochleas are severely dysplastic, so much so that its trilaminar structure is not discernible (Fig. 5B). Concomitant is a 60 to 75% decline in *Kcnq1* message (Table 1) and sparse protein localization on the luminal surface of the marginal cells (Fig. 5D). KCNQ1 is a K^+ ion channel protein that is critical to normal endolymph production and, thus, the integrity of endolymphatic spaces in the cochlea. Loss of functional KCNQ1 K^+ channels results in human and mouse deafness associated with compromised production of endolymph, including the eventual contraction of the SM, collapse of Reissner's membrane, atrophy of the stria vascularis, and degeneration of the organ of Corti and spiral ganglion (Casimiro et al., 2001; Rivas and Francis, 2005).

The stria vascularis of mCMV-infected cochleas is also characterized by dysmorphic and insufficient numbers of melanocytes (Fig. 5B). Intermediate layer melanocytes are essential for normal hearing and melanocyte abnormality results in hearing loss (Schrott and Spoendlin, 1987; Steel and Barkway, 1989; Cable et al., 1992; Peters et al., 1995;

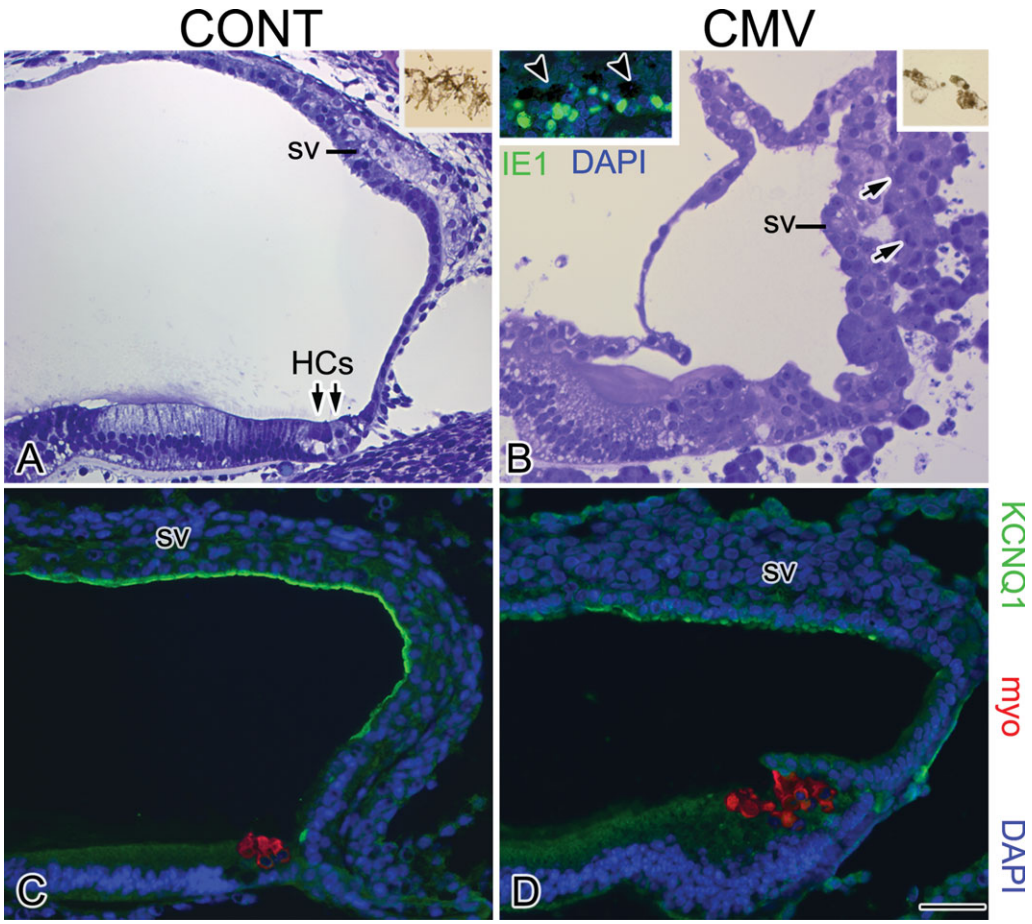

Figure 5. Mouse cytomegalovirus (mCMV)-induced abnormalities in the stria vascularis. (**A, B**) Histologic analysis of semithin plastic sections of control (**A**) and mCMV-infected (**B**) embryonic day 15 (E15) + 12 cochleas. In control (**A**), the stria vascularis (sv) is composed of marginal, intermediate, and basal cells, with melanocytes in the intermediate layer exhibiting a normal phenotype (**A**, inset). With mCMV infection (**B**), the stria vascularis is severely dysmorphic, comprised of enlarged marginal, intermediate and basal cells. Dysmorphic and fewer melanocytes characterize mCMV-infected cochleas (right inset). Note the pathognomonic kidney shaped nuclei (*black arrows*) throughout the stria vascularis, as well as immunodetectable IE1 protein in marginal cells (**B**, left inset) adjacent to abnormal melanocytes (*black arrowheads*, left inset). (**C, D**) Evaluation of KCNQ1 and myosin expression in control and mCMV-infected E15 + 12 cochleas. KCNQ1 protein is labeled green; hair cells are labeled red with an antibody to myosin (myo); nuclei are stained with DAPI (blue). In controls (**C**), KCNQ1 is abundantly present at the luminal surface of the marginal cells of the stria vascularis. In contrast, mCMV-infected cochleas (**D**) show a marked decrease in immunolocalized KCNQ1 protein, exhibiting a punctate labeling pattern. Bar: (**A, B**)-50 μm; (**C, D**)-30 μm; (**B**, left inset) 35 μm; (**A, B**, right insets) 50 μm.

Tachibana, 1999; Uehara et al., 2009). The cell and molecular functions of cochlear melanocytes is not certain. What is known is that melanocytes are required for normal stria vascularis development and function, including mediating the organizational relationship of marginal and basal cells in the trilaminal stria structure, and ion regulation and transport (Steel and Barkway, 1989; Cable et al., 1992; Tachibana, 1999; Bush and Simon, 2007).

To summarize, we describe an in vitro embryonic mouse model of CMV-induced cochlear pathogenesis that mimics the known human pathology. There are several key abnormalities, any one of which would result in deafness at birth or shortly thereafter, including hyperplasia and disorganization of hair and supporting cells in the organ of Corti, as well as stria vascularis dysplasia with concomitant KCNQ1 downregulation and melanocyte hypoplasia and dysmorphia. This is consistent with the emerging understanding that viruses intrinsically depend on their host cells to replicate, assemble, and propagate, they elicit cell and molecular pathologic phenotypes similar to those arising from known gene mutations (Gulbahce et al., 2012; Rozenblatt–Rosen et al., 2012). Thus, the model presented here provides a relevant and reliable platform within which the detailed cell and molecular biology of CMV-induced deafness may be studied.

ACKNOWLEDGMENTS

We thank Dr. Edward Mocarski for his generous gift of *lacZ*-tagged mCMV RM427+ and IE1 antibody.

REFERENCES

Barbi M, Binda S, Caroppo S, et al. 2003. A wider role for congenital cytomegalovirus infection in sensorineural hearing loss. Pediatr Infect Dis 22:39–42.

Baskar JF, Furnari B, Huang ES. 1993. Demonstration of developmental anomalies in mouse fetuses by transfer of murine cytomegalovirus DNA-injected eggs to surrogate mothers. J Infect Dis 167:1288–1295.
Baskar JF, Peacock J, Sulik KK, Huang ES. 1987. Early-stage developmental abnormalities induced by murine cytomegalovirus. J Infect Dis 155:661–666.
Baskar JF, Stanat SC, Sulik KK, Huang ES. 1983. Murine cytomegalovirus-induced congenital defects and fetal maldevelopment. J Infect Dis 148:836–843.
Bush WD, Simon JD. 2007. Quantification of Ca(2+) binding to melanin supports the hypothesis that melanosomes serve a functional role in regulating calcium homeostasis. Pigment Cell Res 20:134–139.
Cable J, Barkway C, Steel KP. 1992. Characteristics of stria vascularis melanocytes of viable dominant spotting (Wv/Wv) mouse mutants. Hear Res 64:6–20.
Cannon MJ, Hyde TB, Schmid DS. 2011. Review of cytomegalovirus shedding in bodily fluids and relevance to congenital cytomegalovirus infection. Rev Med Virol 21:240–255.
Casimiro MC, Knollmann BC, Ebert SN, et al. 2001. Targeted disruption of the Kcnq1 gene produces a mouse model of Jervell and Lange-Nielsen Syndrome. Proc Natl Acad Sci U S A 98:2526–2531.
Cheeran MC, Lokensgard JR, Schleiss MR. 2009. Neuropathogenesis of congenital cytomegalovirus infection: disease mechanisms and prospects for intervention. Clin Microbiol Rev 22:99–126.
Chen P, Segil N. 1999. p27(Kip1) links cell proliferation to morphogenesis in the developing organ of Corti. Development 126:1581–1590.
Chen P, Zindy F, Abdala C, et al. 2003. Progressive hearing loss in mice lacking the cyclin-dependent kinase inhibitor Ink4d. Nat Cell Biol 5:422–426.
Davis GL. 1979. Congenital cytomegalovirus and hearing loss: clinical and experimental observations. Laryngoscope 89(10 Pt 1):1681–1688.
Davis GL. 1981. In vitro models of viral-induced congenital deafness. Am J Otol 3:156–160.
Davis GL, Hawrisiak MM. 1977. Experimental cytomegalovirus infection and the developing mouse inner ear: in vivo and in vitro studies. Lab Invest 37:20–29.
Davis GL, Spector GJ, Strauss M, Middlekamp JN. 1977. Cytomegalovirus endolabyrinthitis. Arch Pathol Lab Med 101:118–121.
Doetzlhofer A, White PM, Johnson JE, et al. 2004. In vitro growth and differentiation of mammalian sensory hair cell progenitors: a requirement for EGF and periotic mesenchyme. Dev Biol 272:432–447.
Driver EC, Kelley MW. 2009. Specification of cell fate in the mammalian cochlea. Birth Defects Res C Embryo Today 87:212–221.
Foulon I, Naessens A, Foulon W, et al. 2008a. A 10-year prospective study of sensorineural hearing loss in children with congenital cytomegalovirus infection. J Pediatr 153:84–88.
Foulon I, Naessens A, Foulon W, et al. 2008b. Hearing loss in children with congenital cytomegalovirus infection in relation to the maternal trimester in which the maternal primary infection occurred. Pediatrics 122:e1123–e1127.
Fowler KB, Boppana SB. 2006. Congenital cytomegalovirus (CMV) infection and hearing deficit. J Clin Virol 35:226–231.
Grosse SD, Ross DS, Dollard SC. 2008. Congenital cytomegalovirus (CMV) infection as a cause of permanent bilateral hearing loss: a quantitative assessment. J Clin Virol 41:57–62.
Gulbahce N, Yan H, Dricot A, et al. 2012. Viral perturbations of host networks reflect disease etiology. PLos Comput Biol 8:e1002531.
Hasson T, Gillespie PG, Garcia JA, et al. 1997. Unconventional myosins in inner-ear sensory epithelia. J Cell Biol 137:1287–1307.
Hasson T, Heintzelman MB, Santos–Sacchi J, et al. 1995. Expression in cochlea and retina of myosin VIIa, the gene product defective in Usher syndrome type 1B. Proc Natl Acad Sci U S A 92:9815–9819.
Hertel L, Chou S, Mocarski ES. 2007. Viral and cell cycle-regulated kinases in cytomegalovirus-induced pseudomitosis and replication. PLoS Pathog 3:e6.
Hertel L, Mocarski ES. 2004. Global analysis of host cell gene expression late during cytomegalovirus infection reveals extensive dysregulation of cell cycle gene expression and induction of Pseudomitosis independent of US28 function. J Virol 78:11988–12011
Jaskoll T, Abichaker G, Jangaard N, et al. 2008a. Cytomegalovirus inhibition of embryonic mouse tooth development: a model of the human amelogenesis imperfecta phenocopy. Arch Oral Biol 53:405–415.
Jaskoll T, Abichaker G, Sedghizadeh PP, et al. 2008b. Cytomegalovirus induces abnormal chondrogenesis and osteogenesis during embryonic mandibular development. BMC Dev Biol 8:33.
Jin Z, Mannström P, Järlebark L, Ulfendahl M. 2007. Malformation of stria vascularis in the developing inner ear of the German waltzing guinea pig. Cell Tissue Res 328:257–270.
Kelley MW. 2007. Cellular commitment and differentiation in the organ of Corti. Int J Dev Biol 51:571–583.
Kern ER. 2006. Pivotal role of animal models in the development of new therapies for cytomegalovirus infections. Antiviral Res 71:164–171.
Kikuchi K, Hilding DA. 1966. The development of the stria vascularis in the mouse. Acta Otolaryngol 62:277–291.
Kirchmaier AL. 2011. Ub-family modifications at the replication fork: regulating PCNA-interacting components. FEBS Lett 585:2920–2928.
Krmpotic A, Bubic I, Polic B, et al. 2003. Pathogenesis of murine cytomegalovirus infection. Microbes Infect 5:1263–1277.
Laine H, Doetzlhofer A, Mantela J, et al. 2007. p19(Ink4d) and p21(Cip1) collaborate to maintain the postmitotic state of auditory hair cells, their codeletion leading to DNA damage and p53-mediated apoptosis. J Neurosci 27:1434–1444.
Li RY, Tsutsui Y. 2000. Growth retardation and microcephaly induced in mice by placental infection with murine cytomegalovirus. Teratology 62:79–85.
Melnick M, Abichaker G, Htet K, et al. 2011. Small molecule inhibitors of the host cell COX/AREG/EGFR/ERK pathway attenuate cytomegalovirus-induced pathogenesis. Exp Mol Pathol 91:400–410.
Melnick M, Mocarski ES, Abichaker G, et al. 2006. Cytomegalovirus-induced embryopathology: mouse submandibular salivary gland epithelial-mesenchymal ontogeny as a model. BMC Dev Biol 6:42.
Melnick M, Phair RD, Lapidot SA, Jaskoll T. 2009. Salivary gland branching morphogenesis: a quantitative systems analysis of the Eda/Edar/NFkappaB paradigm. BMC Dev Biol 9:32.
Moldovan GL, Pfander B, Jentsch S. 2007. PCNA, the maestro of the replication fork. Cell 129:665–679.
Myers EN, Stool S. 1968. Cytomegalic inclusion disease of the inner ear. Laryngoscope 78:1904–1915.
Nance WE, Lim BG, Dodson KM. 2006. Importance of congenital cytomegalovirus infections as a cause for pre-lingual hearing loss. J Clin Virol 35:221–225.
Pass RF. 2007. Congenital cytomegalovirus infection: impairment and immunization. J Infect Dis 195:767–769.
Pass RF, Fowler KB, Boppana SB, et al. 2006. Congenital cytomegalovirus infection following first trimester maternal infection: symptoms at birth and outcome. J Clin Virol 35:216–220.
Peters TA, Kuijpers W, Tonnaer EL, et al. 1995. Distribution and features of melanocytes during inner ear development in pigmented and albino rats. Hear Res 85:169–180.
Puligilla C, Kelley MW. 2009. Building the world's best hearing aid; regulation of cell fate in the cochlea. Curr Opin Genet Dev 19:368–373.
Rarey KE, Davis LE. 1993. Temporal bone histopathology 14 years after cytomegalic inclusion disease: a case study. Laryngoscope 103:904–909.
Rivas A, Francis HW. 2005. Inner ear abnormalities in a Kcnq1 (Kvlqt1) knockout mouse: a model of Jervell and Lange–Nielsen syndrome. Otol Neurotol 26:415–424.
Rosenthal LS, Fowler KB, Boppana SB, et al. 2009. Cytomegalovirus shedding and delayed sensorineural hearing loss: results from longitudinal follow-up of children with congenital infection. Pediatr Infect Dis J 28:515–520.
Rozenblatt–Rosen O, Deo RC, Padi M, et al. 2012. Interpreting cancer genomes using systematic host network perturbations by tumour virus proteins. Nature 487:491–495.
Ruben RJ. 1967. Development of the inner ear of the mouse: a radioautographic study of terminal mitoses. Acta Otolaryngol Suppl 220:1–44.
Schleiss MR. 2006. Nonprimate models of congenital cytomegalovirus (CMV) infection: gaining insight into pathogenesis and prevention of disease in newborns. ILAR J 47:65–72.
Schleiss MR. 2008. Comparison of vaccine strategies against congenital CMV infection in the guinea pig model. J Clin Virol 41:224–230.
Schleiss MR, Choo DI. 2006. Mechanisms of congenital cytomegalovirus-induced deafness. Drug Discov Today 3:105–113.
Schrott A, Spoendlin H. 1987. Pigment anomaly-associated inner ear deafness. Acta Otolaryngol 103:451–457.
Schuknecht HF. 1993. Pathology of the ear. Philadelphia: Lea and Febiger.
Stagno S, Reynolds DW, Amos CS, et al. 1977. Auditory and visual defects resulting from symptomatic and subclinical congenital cytomegaloviral and toxoplasma infections. Pediatrics 59:669–678.
Steel KP, Barkway C. 1989. Another role for melanocytes: their importance for normal stria vascularis development in the mammalian inner ear. Development 107:453–463.
Strauss M. 1990. Human cytomegalovirus labyrinthitis. Am J Otolaryngol 11:292–298.
Tachibana M. 1999. Sound needs sound melanocytes to be heard. Pigment Cell Res 12:344–354.

Teissier N, Delezoide AL, Mas AE, et al. 2011. Inner ear lesions in congenital cytomegalovirus infection of human fetuses. Acta Neuropathol 122:763–774.

Togashi H, Kominami K, Waseda M, et al. 2011. Nectins establish a checkerboard-like cellular pattern in the auditory epithelium. Science 333:1144–1147.

Tsutsui Y. 1995. Developmental disorders of the mouse brain induced by murine cytomegalovirus: animal models for congenital cytomegalovirus infection. Pathol Int 45:91–102.

Tsutsui Y, Kosugi I, Kawasaki H. 2005. Neuropathogenesis in cytomegalovirus infection: indication of the mechanisms using mouse models. Rev Med Virol 15:327–345.

Uehara S, Izumi Y, Kubo Y, et al. 2009. Specific expression of Gsta4 in mouse cochlear melanocytes: a novel role for hearing and melanocyte differentiation. Pigment Cell Melanoma Res 22:111–119.

Van de Water TR, Represa J. 1991. Tissue interactions and growth factors that control development of the inner ear. Neural tube-otic anlage interaction. Ann N Y Acad Sci 630:116–128.

Van de Water TR, Ruben RJ. 1971. Organ culture of the mammalian inner ear. Acta Otolaryngol 71:303–312.

Vollmer B, Seibold–Weiger K, Schmitz–Salue C, et al. 2004. Postnatally acquired cytomegalovirus infection via breast milk: effects on hearing and development in preterm infants. Pediatr Infect Dis J 23:322–327.

von Bohlen und Halbach O. 2011. Immunohistological markers of proliferative events, gliogenesis, and neurogenesis within the adult hippocampus. Cell Tissue Res 345:1–19.

Woolf NK. 1991. Guinea pig model of congenital CMV-induced hearing loss: a review. Transplant Proc 23(3 Suppl 3):32–34, discussion 34.

Xu H, Chen L, Baldini A. 2007. In vivo genetic ablation of the periotic mesoderm affects cell proliferation survival and differentiation in the cochlea. Dev Biol 310:329–340.

Zacchetti A, van Garderen E, Teske E, et al. 2003. Validation of the use of proliferative markers in canine neoplastic and non-neoplastic tissues: comparison of KI-67 and proliferating cell nuclear antigen (PCNA) expression versus in vivo bromodeoxyuridine labelling by immunohistochemistry. APMIS 111:430–438.